Scaling Laws in Side-Chain Liquid Crystalline Polymers: Experimental Evidence of Main-Chain Layer Hopping in the Smectic Phase

L. Noirez,[1] C. Boeffel,[2] and A. Daoud-Aladine[1]
[1]*Laboratoire Léon Brillouin (CEA-CNRS), CE-Saclay, 91191 Gif-sur-Yvette, France*
[2]*MPI für Polymerforschung, Postfach 3148, D-6500 Mainz, Germany*

(Received 19 August 1997)

The average dimensions and the anisotropy of the main chain of a side-chain liquid crystalline polymer are determined in the different mesophases on a series of five different molecular weights. From the comparison of the main-chain dimensions, one deduces that the main chains adopt nearly a self-avoided walk in the isotropic phase. In the smectic phase, the walk adopted between mesogen layers tends to a Gaussian walk, whereas a rodlike behavior is found in the direction parallel to the mesogens. [S0031-9007(97)05212-5]

PACS numbers: 61.30.Jf, 61.12.Ex

In side-chain liquid crystalline polymers, the liquid crystalline properties usually come from the side-chain moieties. The main chain is an ordinary polymer such as a polymethacrylate, a polysiloxane, etc. However, it has been demonstrated many times [1] that the main chain no longer shows a typical polymer behavior since the three-dimensional random conformation resulting from its isotropic entropy is lost. Actually, the main chain is able to adopt either a prolate or an oblate conformation depending on the symmetry of the phase and the nature of the fluctuations which take place [2]. In all cases, the main-chain conformation is deeply affected by the liquid-crystalline field. In other words, the side-chain hinges act along the main chain over distances less than the persistence length. This also means that a total decoupling proceeding from the spacer [3] is not needed to enable the mesomorphy. In the smectic phase, it has been experimentally demonstrated that the main chains occupy preferentially the space between the mesogenic layers [4], confirming what was stated by the theoretical models [5]. In contrast, there is, until now, no element which confirms that the main-chain crossings are defects [5(c)] or layer hoppings [5(a)] (Fig. 1). As for the main chains which are supposed to remain between the mesogen layers, the problem to know what sort of walk is adopted by the polymer main chains remains open. Rieger [5(c)] examined three extreme cases (rodlike, Gaussian, and self-avoided walk) and showed that, in these cases, the solutions should provide nearly the same main-chain anisotropy. Different experimental attempts have led to opposite interpretations. Duran and co-workers [6] are in favor of a fully rigid rodlike main-chain conformation. The main chains are packed in ribbons parallel to the smectic layers and the mesogens hang on one side of the polymer main chain (syndiotactic structure) leading to a rectilinear main-chain conformation. NMR experiments carried out in a frozen smectic phase confirm a strong alignment of the main chains perpendicular to the mesogens [7]. In contrast, other experimental studies carried out by neutron scattering in the intermediate scattering range seem to be in better agreement with a random walk within the smectic plane [8].

In this paper, we give the very first experimental investigations on the main-chain statistics of side-chain liquid crystalline polymers. Small-angle neutron scattering (SANS) is the only method able to provide information on the conformation and anisotropy of oriented chains in the bulk. We give a systematic description of the evolution of the main-chain conformation as a function of the molecular weight (on the basis of five different molecular weights). From this evolution, we deduce that the liquid crystalline field affects strongly the chain statistics. In particular, we demonstrate that the main chain adopts a random walk within the smectic planes where it behaves as a rod through the layers.

The LC polymers used here are the same as described in [1(a)] and corresponds to the structural formula

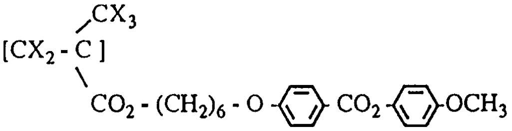

with either $X = \mathrm{H}$ or $X = \mathrm{D}$ (a 1:1 isotopic mixture is used in order to show the appearance of the central scattering associated to the main-chain form factor).

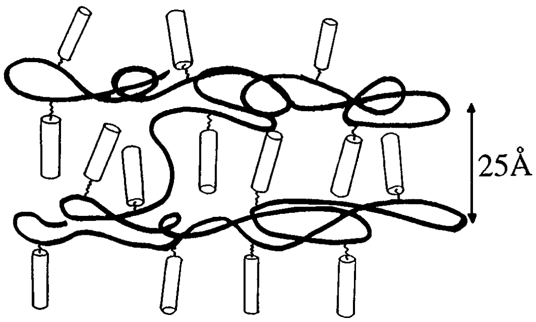

FIG. 1. Hypothetic crossing (defect) of the main chain through the smectic layer. The director is vertical.

Five molecular weight fractions were extracted from the initial batch (obtained by radicalar polymerization) for each H and D species. The polydispersity (determined by gel permeation chromatography) and the molecular weights (determined by absolute calibration of the neutron experiments) are listed below. The same mesophase sequence was observed on the five fractions, with a regular increase of the transition temperatures as a function of the molecular weight: T_g—(25–35 °C)—S_{A1}(smectic)—(64–75 °C)—N(nematic)—(102–111 °C)—I(isotropic).

The smectic phase has been sometimes misidentified [1(a)] because of a lack of typical smectic texture and of a weak specific heat change at the nematic-smectic transition. This transition is much more visible on the fractional samples because of the low polydispersity.

The H:D isotopic mixtures were obtained by evaporation from a solution. The mixed samples were then molten between two quartz windows spaced by 1 mm. In order to proceed to the alignment of the liquid crystalline phases and to the simultaneous SANS measurements, each sample was placed in an oven itself placed between the poles of a magnet of 1.4 T [6]. All samples were submitted to the same thermal history. They were heated up to the isotropic phase, then the temperature slowly decreased (5 °C/h) from the isotropic-nematic transition down to the smectic phase while the scattered signal was measured as referred in [9]. The resulting transparency indicates that the alignment process was achieved in the nematic phase and the presence of a well-defined 001 reflection at low temperature (easily visible on the fully hydrogenated sample since the absence of central scattering) indicates a monolayer smectic phase of 25 Å thickness [9].

The scattered beam was collected on the plane of the two-dimensional spectrometer (PAXY of the Laboratoire Léon Brillouin) using two settings to cover the small-angle range corresponding to the Guinier domain ($qRg \leq 1$). For low molecular weights, we explored a q range (where q is the scattering vector defined by $q = (4\pi/\lambda)\sin(\theta/2)$, where λ is the wavelength and θ is the scattering angle) of 0.008 to 0.08 Å^{-1}. For high molecular weights, the wavelength was switched up from 10 to 14 Å providing a q range of 0.006 to 0.06 Å^{-1} (diffraction measurements have been carried out at $\lambda = 5$ Å). The data were normalized and the (incoherent and electronic) backgrounds removed.

At small angles, the signal obeys the Zimm approximation for which the scattered intensity $S(q)$ is proportional to the form factor $P(q)$ associated with the main-chain part of the polymer:

$$S(q)\alpha P(q) = 1/\langle 1 + (R_x^2 q_x^2 + R_y^2 q_y^2 + R_z^2 q_z^2)\rangle,$$

$$\text{with } R_g^2 = R_x^2 + R_y^2 + R_z^2 .$$

Let us choose O_x as the axis parallel to the magnetic field: $R_x = R_\parallel$ and $R_y = R_z = R_\perp$ are the components of the radius of gyration R_g of the polymer main chain following and perpendicular to the director, respectively (only one perpendicular component is measured in the multidetector plane).

We used a two-dimensional fit to extract $R_\parallel$ and $R_\perp$ from the two-dimensional Lorentzian $P(q_\parallel, q_\perp)$ [10]. This procedure presents the huge advantage of avoiding the systematic error introduced by the traditional use of masks of defined widths, and also increases considerably the statistics. The extra scattering, likely due to catalyst heterogeneities (Fig. 2), is also fitted extending the Guinier domain to the lowest angles. After calibration of the incident neutron beam, the scattered intensity $S(q)$ is normalized as described in [11]. The molecular weight M_W of each H:D mixture, deduced (with an accuracy of 5%) from the intensity at zero-q value, are the following: $M_W(1) = 76\,500$, $M_W(2) = 142\,000$, $M_W(3) = 270\,000$, $M_W(4) = 382\,000$, $M_W(5) = 870\,000$, with the corresponding polydispersity: $I(1) = 1.66$, $I(2) - 1.32$, $I(3) = 1.29$, $I(4) = 1.25$, $I(5) = 1.33$. Figure 3 shows the evolution of the main-chain anisotropy for each molecular weight species as a function of the temperature. The following features can be deduced.

(i) In the isotropic phase, $R_\parallel$ and $R_\perp$ are systematically confused within the error bars; the polymer main chains are isotropically distributed.

(ii) In the nematic phase, a slight main-chain anisotropy is observed ($R_\parallel \leq R_\perp$). The extension of the polymer main chain perpendicular to the director ($R_\perp$) shows a weak increase compared to the isotropic state, whereas the parallel extension ($R_\parallel$) is significantly reduced. The main chains tend to be mostly perpendicular to the director.

(iii) As soon as the nematic-smectic A transition, the anisotropic oblate shape is asserted. It results essentially from a strong reduction of the extension $R_\parallel$ to the director. Actually, the behavior observed in the smectic phase corresponds to a local microsegregation of the main chains between the layers formed by the side mesogens [4]. It is interesting to remark on Fig. 3 that the difference $\Delta = (R_\parallel - R_{\text{iso}})$ remains approximately constant. The invariance of Δ and its value (≈20–25 Å) close to the

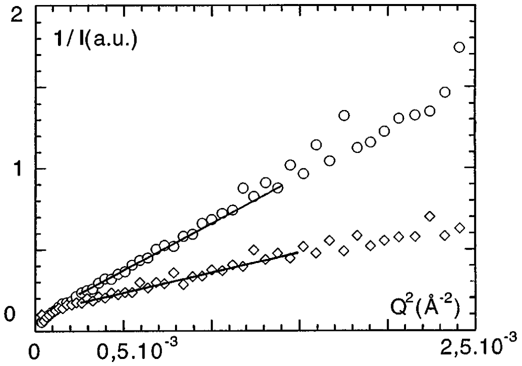

FIG. 2. Zimm representation of the intensity scattered in the parallel (◇) and the perpendicular axis (○) to the director by the polymer of mass $M_W(4) = 382\,000$ at 65 °C.

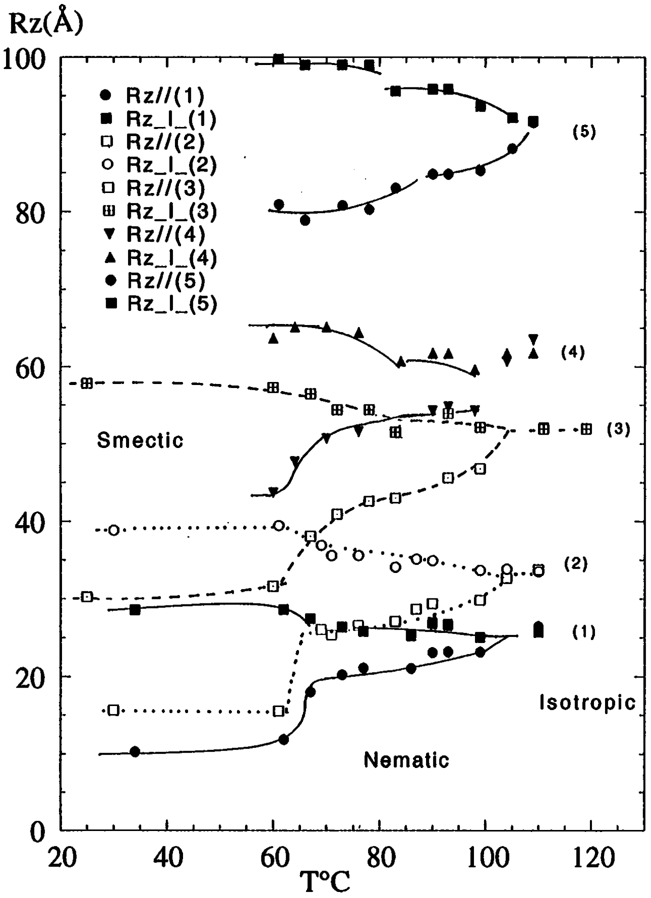

FIG. 3. Evolution of the components parallel and perpendicular to the director $\langle R_{\parallel} \rangle_z$ and $\langle R_{\perp} \rangle_z$ of the radius of gyration of the main chain versus temperature for each molecular weight (continuous lines are only guides for eyes).

smectic layer thickness (25 Å) could indicate that there is no decorrelation between confined main-chain layers. At last, just on the basis of the evolution of the main-chain conformation, three different regimes corresponding to the three different phases can be identified.

A convenient way to describe the walk adopted by a polymer chain is to establish the relation which relies on the chain dimension to its degree of polymerization N: $R_g^2 = b_0^2 N^{2\nu}/6$, where b_0 is the statistical unit and ν is a critical exponent depending on the excluded volume. This relation supposes that R_g and N describe the same average which is realized when the polydispersity I is low [the scattering experiments give the weight average molecular weight (M_W) and the z-average radius of gyration ($\langle R_g^2 \rangle_z$)]. This condition is fulfilled here in first approximation since $I \approx 1.3$. The values corrected from polydispersity, indicated in brackets, are calculated with the formula appropriated to each supposed walk [12] and correspond to an equivalent monodisperse weight average. These corrections affect mostly the prefactor.

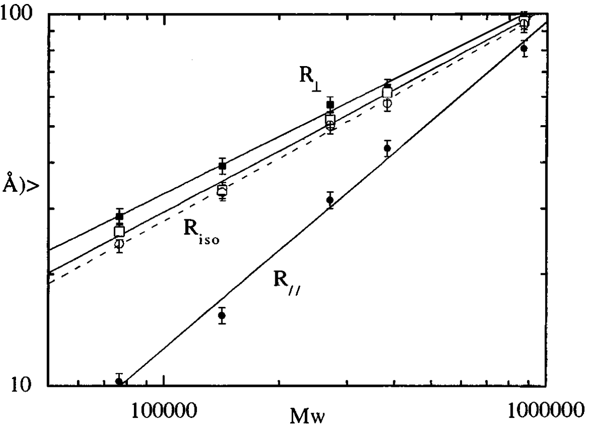

FIG. 4. Log-log dependence versus M_w of $\langle R_{\mathrm{iso}} \rangle_z$ (□), $\langle R_{\parallel} \rangle_z$ (●), and $\langle R_{\perp} \rangle_z$ (■). $\langle R_{\mathrm{SA}} \rangle_z = [\frac{1}{3}\langle R_{\parallel}^2 \rangle + 2\langle R_{\perp}^2 \rangle)]^{0.5}$ (○) corresponds to the unoriented average size in the smectic phase (dotted line).

In the isotropic phase (Fig. 4), the main-chain walk is described by $\langle R_{\mathrm{iso}}^2 \rangle^{1/2} = (0.056 \pm 0.012) M_w^{0.54 \pm 0.02}$, where $\nu_{\mathrm{iso}} = \nu_{\parallel} = \nu_{\perp} \approx 0.54 \pm 0.02$ [and $R_{\mathrm{iso}_W} = (0.046 \pm 0.011) M_w^{0.55 \pm 0.02}$]. This exponent is intermediate between a Gaussian behavior (in the bulk $\nu = 0.5$) and a self-avoiding walk (in a good solvent $\nu = 0.58$). The expected value would be $\nu = 0.5$, since the isotropic phase is the "less" mesomorphic phase. However, only the main-chain behavior is considered and lateral mesogens could procure a kind of dilution contributing to excluded volume effects.

In the smectic phase, the main-chain behavior is deeply different following the directions parallel and perpendicular to the director. Figure 4 represents, in logarithmic scale, the evolution of the extensions $R_{\parallel}$ and $R_{\perp}$ of the main chain at 63 °C versus molecular weight. In the perpendicular direction (within the smectic planes), we obtain $\langle R_{\perp}^2 \rangle_z^{1/2} = (0.095 \pm 0.022) M_w^{0.51 \pm 0.02}$ with $\nu_{\perp} \approx 0.51 \pm 0.02$ [with the polydispersity corrections: $R_{\perp_w} = (0.078 \pm 0.020) M_w^{0.51 \pm 0.02}$]. This law describes the main chains confined between two successive mesogenic layers. Two antagonistic effects appear in these main-chain sublayers. The first is a nearness of the main chains since the repulsive interactions with the mesogens stacked into the layers decrease. The second effect is a consequence of the confinement which forces the chains to a two-dimensional walk. The reduction of dimensionality should increase excluded volume interactions. The experimental observation seems to be in favor of the first argument probably because, even confined, the main chains still occupy enough place to keep a three-dimensional walk. In this case, the main chains separated from their undesirable side parts are stacked close to each other and, thus, show a typical Gaussian behavior. This result is in agreement with the very first observations carried out in the intermediate scattering range [8]. In the direction parallel to the director (we examine the layer crossings), we obtain $\langle R_{\parallel}^2 \rangle_z^{1/2} = (1.10^{-3} \pm 5 \times 10^{-4}) M^{0.83 \pm 0.03}$ [corrected from polydispersity: $R_{\parallel_w} = (1, 2.10^{-3} \pm 5 \times 10^{-4}) M_w^{0.83 \pm 0.03}$]. This behavior is the signature of an extreme situation of excluded volume; main chains are remote from each other. It is a rodlike behavior. This is the first experimental evidence of the existence of a rodlike behavior through the smectic layers. The notion of layer defects introduced by the theoreticians [5] fits completely with the experimental observation.

Using the information exposed above, we can investigate, in more detail, the statistics of the main chain in the smectic phase by determining the statistical unit length in both directions as well as the ratio of chain length involved in the crossings. Through the layers:

$$R_\parallel^2 = b_\parallel^2 N_\parallel^{2\nu_\parallel}/6 \qquad \text{with } 2\nu_\parallel = 1.66 \pm 0.08\,; \tag{1a}$$

in the layer plane:

$$(R_y^2 + R_z^2) = 2R_\perp^2 = b_\perp^2 N_\perp/6 \qquad \text{since } 2\nu_\perp = 1\,, \tag{1b}$$

where $N_\parallel$ and $N_\perp$ are, respectively, the number of independent steps in the directions parallel and perpendicular to the mesogens, and $b_\parallel$ and $b_\perp$ are the corresponding statistical units. Since the main-chain crossings behave as a rod, we can approximate $b_\parallel$ to the layer thickness (25 Å) [5(b)] and deduce $N_\parallel$, the number of crossings per chain, from the relation (1). We found $N_\parallel \approx 4$ for the polymer $M_W(2)$. This quantity varies by definition linearly with N. The ratio $\rho = N_\parallel b_\parallel / L$, where L is the total contour length of the chain ($L = N_\parallel b_\parallel + N_\perp b_\perp$), gives an idea of the proportion of the chain length which is crossings. ρ is about 6% of the total length. It means that the microsegregation effect is very efficient. Finally, from the knowledge of $R_\perp$, $b_\parallel$, $N_\parallel$, and L, we estimate $b_\perp = 22 \pm 3$ Å in the smectic plane. This value is not far from the isotropic phase ($b_0 = 15 \pm 2$ Å), and remains coherent with flexible Gaussian chains. Figure 4 shows also the mass dependence of the unoriented average size $\langle R_{\mathrm{SA}} \rangle$ in the smectic phase (dotted line). Its similarity with the curve obtained in the isotropic state is remarkable and reveals a likely identical local state. Finally, this study would not be complete without mentioning the behavior in the nematic phase. The variation of $R_\parallel$ and $R_\perp$ at 85 °C gives, respectively, $R_\parallel^2 \alpha M_w^{1.16 \pm 0.04}$ and $R_\perp^2 \alpha M_w^{1.08 \pm 0.04}$. This behavior, intermediate between the isotropic and the smectic phase, is very likely dominated by the smectic fluctuations present in the whole nematic phase. The study of a “real” nematic polymer exempt of smectic fluctuations is needed to appreciate the main-chain behavior in this phase.

In conclusion, this study has shown that a complete change of the main-chain behavior occurs in the smectic phase depending on whether the chain crosses or remains within the mesogenic layers. The walk adopted by the main chains through the mesogenic layers is very close to a rodlike walk. This is in very good agreement with the notion of defects introduced by the theoreticians. The nematic “hairpin” model introduced by de Gennes some years ago to characterize the defects of nematic linear polymers [13] found its analog in smectic side-chain polymers with the main-chain layer hoppings. Both are issued from a reduction of the chain entropy resulting from the liquid crystalline field and correspond to localized and solitary defects. Within the smectic planes, the main chain shows a nonforeseeable Gaussian behavior. This return to a bulk behavior can be explained if we consider that the side-chain mesogens are at the origin of the excluded volume. This result is also consistent with the behavior noticed in the isotropic phase. However, these measurements have been carried out just above the nematic-isotropic transition and the influence of the neighboring mesophase is perhaps not negligible in the self-avoided walk behavior observed in the isotropic phase. Finally, since the molecular weight affects much more the rodlike behavior than a Gaussian one, the extrapolation of these distinct behaviors to the high molecular weights should reveal a change of anisotropy of conformation. Such a transition remains to be discussed and observed.

The authors are very grateful to W. Stocker and V. Abetz who gave their assistance during the neutron experiments in Saclay in November 1993, and Uta Pawelzik for her help in the polymer synthesis.

[1] (a) R. G. Kirste and H. G. Ohm, Makromol. Chem. Rapid. Commun. **6**, 179 (1985); (b) P. Keller *et al.,* J. Phys. Lett. **46**, 1065 (1985).

[2] L. Noirez *et al.*, J. Phys. (Paris) **49**, 1993 (1988).

[3] H. Finkelmann *et al.*, Makromol. Chem. **179**, 273 (1987).

[4] H. G. Ohm *et al.,* Makromol. Chem. **116**, 1387 (1988); V. A. Gudkov, Sov. Phys. Crystallogr. **29**, 316 (1984); P. Davidson and A. M. Levelut, Liq. Cryst. **11**, 469 (1992); L. Noirez *et al.,* Liq. Cryst. **16**, 1081 (1994).

[5] (a) W. Renz and M. Warner, Phys. Rev. Lett. **56**, 1268 (1986); (b) A. B. Kunchenko and D. A. Svetogorsky, J. Phys. (Paris) **47**, 2015 (1986); (c) J. Rieger, J. Phys. (Paris) **49**, 1615 (1988).

[6] R. Duran *et al.*, J. Phys. (Paris) **49**, 1455 (1988); **48**, 2043 (1987).

[7] C. Boeffel and H. W. Spiess, Macromolecules **21**, 1626 (1988).

[8] L. Noirez, J. P. Cotton, and P. Keller, Liq. Cryst. **18**, 129 (1995).

[9] L. Noirez, P. Keller, and J. P. Cotton, J. Phys. II (France) **2**, 915 (1992).

[10] G. Pépy, program “PXY” available at the Laboratoire Léon Brillouin.

[11] J. P. Cotton, *Neutron, X-Ray and Light Scattering,* edited by P. Lindner and T. Zemb (North-Holland, Amsterdam, 1991).

[12] R. C. Oberthür, Makromol. Chem. **179**, 2693 (1978).

[13] P. G. de Gennes, *Polymer Liquid Crystals*, edited by A. Ciferri, W. R. Krigbaum, and R. B. Meyer (Academic, New York, 1982).